Archives of Biochemistry and Biophysics 772 (2025) 110557

Contents lists available at ScienceDirect

Archives of Biochemistry and Biophysics

journal homepage: www.elsevier.com/locate/yabbi

Ubiquitous calpains show differential dynamics and function during adipocyte differentiation

L. Rodríguez-Fernández [a], R. Zaragozá [b,c], J.R. Viña [a,b], E.R. García-Trevijano [a,b,*]

[a] Departamento de Bioquímica y Biología Molecular, Facultad de Medicina. Universidad de Valencia, Spain
[b] Fundación Investigación Hospital Clínico-Incliva. Valencia, Spain
[c] Departamento de Anatomía y Embriología Humana. Facultad de Medicina. Universidad deValencia, Spain

ARTICLE INFO

Keywords:
Nuclear calpain-1
Calpain-2
Histone H3
3T3-L1-differentiation
Cleavage

ABSTRACT

Adipose tissue homeostasis is disrupted either, by decreased adipocyte number or increased adipogenesis, leading to endocrine dysfunction, developmental anomalies, or tumour progression. Calpains are calcium-dependent proteases that modulate adipogenesis, yet the distinct roles of ubiquitously expressed isoforms calpain-1 (CAPN1) and calpain-2 (CAPN2) remain unclear. This study investigates calpains isoform- and phase-specific expression, distribution, and function during hormonally induced 3T3-L1 preadipocyte differentiation. Both isoforms showed progressive upregulation, increased activity (Nt/Ct-CAPN1 ratio, calpastatin levels and enzymatic activity), and dynamic isoform-specific redistribution throughout differentiation phases. Depletion of CAPN1 or CAPN2 disrupted the transition from mitotic clonal expansion (MCE) to early differentiation (ED) stage, preventing cell cycle exit, as indicated by impaired C/EBPα expression, increased S-phase preadipocytes, and elevated p53 levels. Immunofluorescence staining revealed distinct N-terminal/C-terminal histone H3 patterns at the MCE-to-ED transition. Calpain inhibition or depletion prevented histone H3 cleavage, and proximity ligation assays confirmed *in vivo* CAPN1/Nt-H3 interaction. Although the precise CAPN2 targets during adipocyte differentiation remain unknown, CAPN1 was identified as the main isoform responsible for chromatin remodelling by histone H3 cleavage at MCE-to-ED transition. These findings underscore the critical role of phase-specific calpains in the adipogenic program, revealing them as potential therapeutic targets for obesity and metabolic disorders.

1. Introduction

Excessive adipose tissue accumulation leads to increased fat storage and obesity, which can cause metabolic and cardiovascular diseases, steatosis, liver cirrhosis, or even cancer [1]. Adipogenesis can be understood as the process of preadipocyte differentiation. During this process, commitment of mesenchymal stem cells (MSCs) to preadipocytes is followed by a set of sequential phases to obtain mature adipocytes, including growth arrest (GA), mitotic clonal expansion (MCE), and early and terminal differentiation (ED and TD) [1]. MSCs are not only precursors to preadipocytes but also give rise to myogenic, osteogenic, and chondrogenic cells [2]. Furthermore, mature adipocytes have the ability to dedifferentiate and subsequently differentiate into different cell types according to tissue needs. Adipocytes surrounding breast tumour cells can also dedifferentiate and transform into fibroblast-like cells with tumour-promoting potential [1,3]. These data highlight the importance for the study of adipocyte differentiation. Unfortunately, the underlying mechanisms for their differentiation program remain not fully understood.

The 3T3-L1 embryonic preadipocyte murine cell line is a well-established model for studying the in vitro-induced adipogenesis. Several cysteine proteases have been reported to play a role in the modulation of cell differentiation, including calpains [4–6].

Calpains are a family of intracellular calcium-dependent cysteine proteases. Among the 15 members of this family, calpain-1 and calpain-2, ubiquitously expressed in mammalian tissues, are the best characterized isoforms for their known role in physiological and pathological processes [7–9]. Both enzymes, are heterodimers consisting of a large ~80 kDa catalytic subunit specific to each isoform (encoded by CAPN1 and CAPN2 genes) and a small ~28 kDa regulatory subunit (encoded by

* Corresponding author. Departamento de Bioquímica y Biología Molecular. Fundación Investigación Hospital Clínico-Incliva, Facultad de Medicina. Universidad de Valencia, Spain Avda. Blasco Ibáñez, 15. 46010 Valencia, Spain. Tel.: 00 34 963983886.
E-mail address: elena.ruiz@uv.es (E.R. García-Trevijano).

https://doi.org/10.1016/j.abb.2025.110557
Received 20 May 2025; Received in revised form 18 July 2025; Accepted 19 July 2025
Available online 21 July 2025

CAPNS1 gene) common to both isoforms [7]. Additionally, completing the calpain axis, calpastatin (encoded by the CAST gene) is the endogenous inhibitor of both calpains [8]. Calpains modify cellular proteins through limited proteolysis, a controlled cleavage process that affects protein function without causing degradation. The cleaved products generated by calpains can differ from the original substrates in terms of function, protein–protein interactions, or subcellular localization [9–12]. This processing ability allows calpains to regulate a broad range of cellular activities.

The calpain axis was the first reported proteolytic system functionally involved in the regulation of adipocyte differentiation [13,14]. In early experiments, the inhibition of calpain activity by chemical inhibitors, or by CAST overexpression, was shown to effectively block the MCE phase of 3T3-L1 cells following *in vitro*-induced differentiation [13,14]. *In vivo* experiments with CAST transgenic mice resulted in reduced adipose tissue macrophage accumulation in obese mice. Furthermore, calpain protein levels and activity were increased in the adipose tissue of these obese mice; calpain inhibition in this model significantly modulated adipose tissue remodelling affecting adipocyte apoptosis, fibrosis, inflammation, and the migratory properties of macrophages [15].

Although substantial evidence confirms the involvement of calpains in adipocyte differentiation, several [16] underlying questions remain to be elucidated, and some data seem contradictory or at least intriguing. The role of calpains was reported to be limited to a window during the MCE phase of embryonic 3T3-L1 preadipocytes [14]. However, the MCE requirement for adipogenesis is controversial [6,16–18]. Some authors suggest that MCE is not required for the full differentiation of adult ST-13 preadipocytes and yet calpains still modulate the differentiation of ST-13 cells [16].

Those early studies on the role of calpains in adipocyte differentiation, although undoubtedly inspiring, were sometimes based on concepts that are now outdated or lacked a comprehensive analysis of calpains dynamics throughout the differentiation of 3T3-L1. Herein, we explored the mechanisms underlying the function and detailed distribution of calpain-1 and calpain-2 during the time-course of adipocyte differentiation, uncovering an important role for nuclear calpains in the epigenetic program of this process.

2. Material and methods

2.1. Materials

Cocktail MDIR to induce differentiation: Insulin and methylisobutylxanthine (Sigma Aldrich) Dexamethasone (G-Biosciences), and rosiglitazone (Cayman Chemical). Primary antibodies for Ct-CAPN1 (ab39170, recognizing latent and aminoprocessed-activated Calpain 1), Nt-CAPN1 (ab28257), β-actin (ab8227), α-tubulin (ab52866) and GAPDH (ab8245) were all from abcam. Other antibodies used in this study were anti-CAPN2 (2539, cell signaling), anti-CAPNS1 (H0000826M1, Sigma-Aldrich), anti-Calpastatin (MA3-944 ThermoFisher Sci), anti-Plin-1 (651156, Progen Bio), anti-(Nt) Histone H3 (39763, Active Motif), anti-(Ct)-histone H3 and anti-Leptin (07-690 and AB1673, respectively both from Merck), anti PPARγ (sc-7273, Santa Cruz Biotechnology) and anti-Fibrillarin (NB300-269, Novus Biologicals). Predeveloped Taqman primers for *capn1* (Mm00482964_m1), *capn2* (Mm00486669_m1), *c/ebpα* (Mm01194587_m1), *plin-1* (Mm00558672_m1), *lep* (Mm00434759_m1) and 18S rRNA Endogenous Control (4319413E) were all from Applied Biosystems. Calpain inhibitors were both from Calbiochem (Merck chemicals): calpeptin (03-34-0051), and ALLN (N-acetyl-L-leucyl-L-leucylnorleucinal; 208719) and recombinant histone H3 were from Merck (14-494).

2.2. Cell culture and differentiation of 3T3-L1

Murine 3T3-L1 fibroblast cell line (ATCC) was maintained in basal medium (high glucose DMEM, Gibco) supplemented with 10 % Bovine Calf Serum, 1 % Penicillin/streptomycin (K952, Amresco) and L-glutamine (G7513, Sigma). Routinely cultured cells never reached confluence. For differentiation experiments, 100 % confluent cells were cultured for 2 additional days and then, differentiation was induced with MDIR (0.5 mM methylisobutylxanthine (IBMX), 1.0 μM dexamethasone, 1.0 μg/mL insulin and 2.0 μM rosiglitazone) as previously described [19]. After 48 h, culture media was replaced by basal media supplemented with 1.0 μg/mL insulin, further cultured for other 48 h and then, media replaced again by basal media. For calpain inhibition experiments, confluent 3T3-L1 pre-adipocytes were treated with 50 μM Calpeptin, 50 μM ALLN or DMSO before the induction of differentiation.

2.3. CAPNs silencing by esiRNA

3T3-L1 cells were reversely-transfected with 30 nM capn1, capn2 small interfering RNA (esiRNA), or Universal Negative Control scRNA (EMU057001-50UG, EMU080871-50UG, SIC001, Sigma) 48 h before the induction of differentiation. Cells were reverse-transfected with Lipofectamine RNAiMAX (13778075, Life Technologies). The transfection reaction was carried out for 24 h. Dilutions of esiRNA and Lipofectamine were performed in Opti-MEM following the manufacturer's instructions. esiRNA transfection efficiency was analysed 72 h after induction of differentiation by RT-PCR or Western blot.

2.4. CAPN activity assay

To measure CAPN activity, we used the 'calpain activity assay kit' (QIA-120, Sigma) that includes Suc-LLVY-AMC as the fluorogenic calpain substrate. 3T3-L1 cells at different phases of differentiation or fully differentiated adipocytes treated with different inhibitors, were solubilized in a cell lysis buffer provided with the kit and protease activity was measured following manufacturer's instructions in a SpectraMAX Gemini fluorometric reader. The CAPN activity was calculated by subtracting the activity observed with a CAPN-inhibition buffer containing BAPTA—a calcium chelator that fully inhibits CAPN—from the activity measured with the activation buffer, which contains calcium and a reducing agent (TCEP).

2.5. Immunofluorescence staining

Cells were cultured onto 13 mm Ø borosilicate Cover Glass (VWR 631-0149) and immunostained as described elsewhere. Briefly, cells were incubated (4 °C o.n.) with the indicated primary antibodies, followed by the secondary antibody. To ensure the signal specificity, a negative control (without primary antibody) was routinely included. Nuclei were counterstained with DAPI (Invitrogen). Images were acquired on a LEICA TCS-SP8 confocal microscope. Fields with too few or too many cells were excluded. At least 4 fields for each independent experiment were analysed. The average number of cells/fields was usually 60 ± 10. Images were analysed using Leica Application Suite X program. The most representative image was always selected.

2.6. Oil red o staining

3T3-L1 cells were pre-treated with CAPN inhibitors (Calpeptin and ALLN) immediately prior to the induction of differentiation and stained with Oil Red O at MCE-to-ED transition. Briefly, cells were washed with PBS and fixed with 10 % formaldehyde/PBS for 45 min. Cells were then washed with distilled water and incubated for 5 min with 60 % isopropanol, followed by 5 min incubation with Oil Red O working solution (3:2, Oil Red O stock solution: Water). Oil Red O stock solution was prepared in isopropanol according to manufacturer's instructions. After several washes with water, cells were stained with haematoxylin, and imaged with a Leica DMI 3000 microscope.

2.7. Proximity ligation assay (PLA)

To detect in situ interaction between the proteins of interest, the Duolink® In Situ assay (DUO92102, Sigma-Aldrich) based on PLA technique was used. 3T3-L1 cells at MCE and ED-TD were selected to study CAPN1/histone H3-Nt and CAPN2/histone H3-Nt interactions. Cells were fixed and permeabilized as described for immunofluorescence (IF) analysis. Following permeabilization, cells were incubated with blocking solution (normal gat serum X0907, Dako) 30 min at 37 °C and incubated with primary antibodies over night at 4 °C. PLA-probe dilutions were added and incubated for 1 h 37 °C. PLA probe ligation and amplification were performed following the manufacturer's instructions. Finally, samples were covered with Duolink In Situ Mounting Medium with DAPI (for nuclei staining) and analysed with a LEICA TCS-SP8 confocal microscope. PLA positive cells were quantified using Duolink ImageTool program.

2.8. Protein extraction and immunoblotting

Total protein was extracted in the presence of protease inhibitors in RIPA buffer as elsewhere described. Equal amounts of protein were size fractionated by SDS–PAGE electrophoresis and electroblotted onto nitrocellulose membranes. The specific proteins were detected using the indicated primary antibodies and HRP-conjugated secondary antibody (DAKO). Blots were developed by enhanced chemiluminescence reaction (ECL Detection Kit, GE Healthcare). Equal loading was confirmed by re-probing the blot against α-tubulin, β-actin or GAPDH and by Ponceau Red staining. For data quantification, Fiji—ImageJ software (www.imagej.net/Fiji) was used. Signal intensity of the protein of interest was divided by the corresponding signal for GAPDH (or β-actin), followed by normalization to its relative control within each experiment (GA phase, scRNA or DMSO treatment). All the original, uncropped Western blot data can be found in Supplementary material.

2.9. Subcellular fractionation

Nuclear and cytosolic fractions were isolated using the Nuclear Extract kit (40010, Active Motif) according to manufacturer's instructions. In brief, washed cells were pelleted and lysed in hypotonic buffer to obtain cytoplasmic fractions. Nuclear pellets were incubated in lysis buffer for 30 min with gentle agitation at 4 °C. Samples were then centrifuged and supernatants recovered as nuclear fractions.

2.10. RT-qPCR

Total RNA from 3T3-L1 cell was extracted (74104, RNeasy, Qiagen) and RNA quantity and purity determined with Nanodrop ND-2000. RNA (500 ng) was reverse-transcribed into cDNA at 37 °C for 60 min and 95 °C for 5 min using a high-capacity RNA-to-cDNA kit (4387406, Applied Biosystems). The cDNA products were amplified by qPCR using the GeneAmp PCR Master mix (4369016, Applied Biosystems). All reactions were carried out in triplicate. qPCR was performed using the 7900HT Fast Real-Time PCR system. Results were normalized according to 18S quantification in the same sample reaction. The threshold cycle (CT) was determined and then the relative gene expression was expressed as: relative amount $= 2^{-\Delta(\Delta CT)}$.

2.11. Flow cytometry

3T3-L1 cells were analysed by flow cytometry at the Cytometry Unit from Unidad Central de Investigación de Medicina (UCIM), Universitat de Valencia. Briefly, cells were transfected with either scRNA, siCAPN1 or siCAPN2 48 h prior to MDIR-induced differentiation. Cells were trypsinized 72 h after transfection, fixed with 70 % ethanol, stained with propidium iodide (P4170, Sigma) and run in a flow cytometer (BD FACS Vosse) using a FACSuite software. Subsequent analysis with ModFit LT (V4.1.7) software was used for cell cycle examination.

2.12. Statistics

The statistical analysis and graph plotting were performed using the Graph pad Prism software v.10.4.1 (LLC, CA, USA.). Data were analysed by One-Way Anova test with multiple comparisons and then by Tukey's test. The results were expressed as mean ± standard deviation, and differences were considered significant when $p < 0.05$ (*), $p < 0.01$ (**), $p < 0.001$ (***) or $p < 0.0001$ (****). Independent experiments were conducted with a minimum of three replicates per condition to allow statistical comparison.

3. Results

3.1. Phase-specific expression of calpain-1 and calpain-2 during the time course of 3T3-L1 differentiation

The 3T3-L1 cell line was used as experimental model to study the expression patterns of calpain-1 and -2 throughout the course of adipocyte differentiation. Data variability among laboratories using this model is believed to result from differences in culture methods. When sub-confluent, proliferating pre-adipocytes are exposed to MDIR, differentiation efficiency may decrease, or the timing of molecular events leading to differentiation may shift [20,21]. Accordingly, to accurately correlate the temporal patterns of calpain expression with function during adipocyte differentiation, we will refer to specific differentiation stages rather than the number of days post-MDIR induction. Thus, it is essential to first identify the distinct stages of 3T3-L1 differentiation.

After MDIR exposure, 3T3-L1 cells undergo progressive morphological changes (Fig. 1A), transitioning from a spindle-shaped, fibroblastic appearance in growth-arrested (GA) pre-adipocytes to a spherical shape characteristic of mature adipocytes at terminal differentiation (TD). Initial stages of early differentiation (ED) were marked by Perilipin-1 (PLIN-1) immunostaining in few lipid droplets, while extensive immunostaining indicated full differentiation at the TD stage [22].

To further characterize key events triggered at the MCE-ED and ED-TD transitions, Plin-1 and leptin mRNA levels were analysed (Fig. 1B). While Plin-1 mRNA levels increased at MCE-ED transition, upregulation of leptin mRNA was not observed until ED-TD stage. As expected, PLIN-1 protein levels increased later than its mRNA, at ED-TD transition (Fig. 1C). Increased PPARγ and leptin protein levels also indicate the completion of differentiation at the TD stage. These data effectively define the timeframe for the MCE to ED transition during 3T3-L1 differentiation.

CAPN-1 and CAPN-2 protein levels were analysed in the same samples (Fig. 1D) to assess whether specific phases of pre-adipocyte differentiation are influenced by CAPN abundance. Protein levels of both, CAPN-1 and CAPN-2 increased progressively throughout differentiation. The onset of CAPNs upregulation was observed during the MCE-ED transition and reached the highest levels at the TD stage.

These findings suggest that both calpains might modulate early and terminal differentiation. However, higher CAPN protein levels do not necessarily indicate increased calpain activity. Therefore, further evidence of calpain activity and subcellular localization should be assessed to stablish their roles in the differentiation of 3T3-L1 cells.

3.2. Phase-specific analysis of calpain activity during 3T3-L1 differentiation

To investigate the stage-specific modulation of calpain activity during the 3T3-L1 differentiation program, evidences of increased enzymatic activity were analysed.

The autolysis of the N-terminal anchor helix, has been considered as an indicator of increased calpain-1 activity [23]. The removal of the

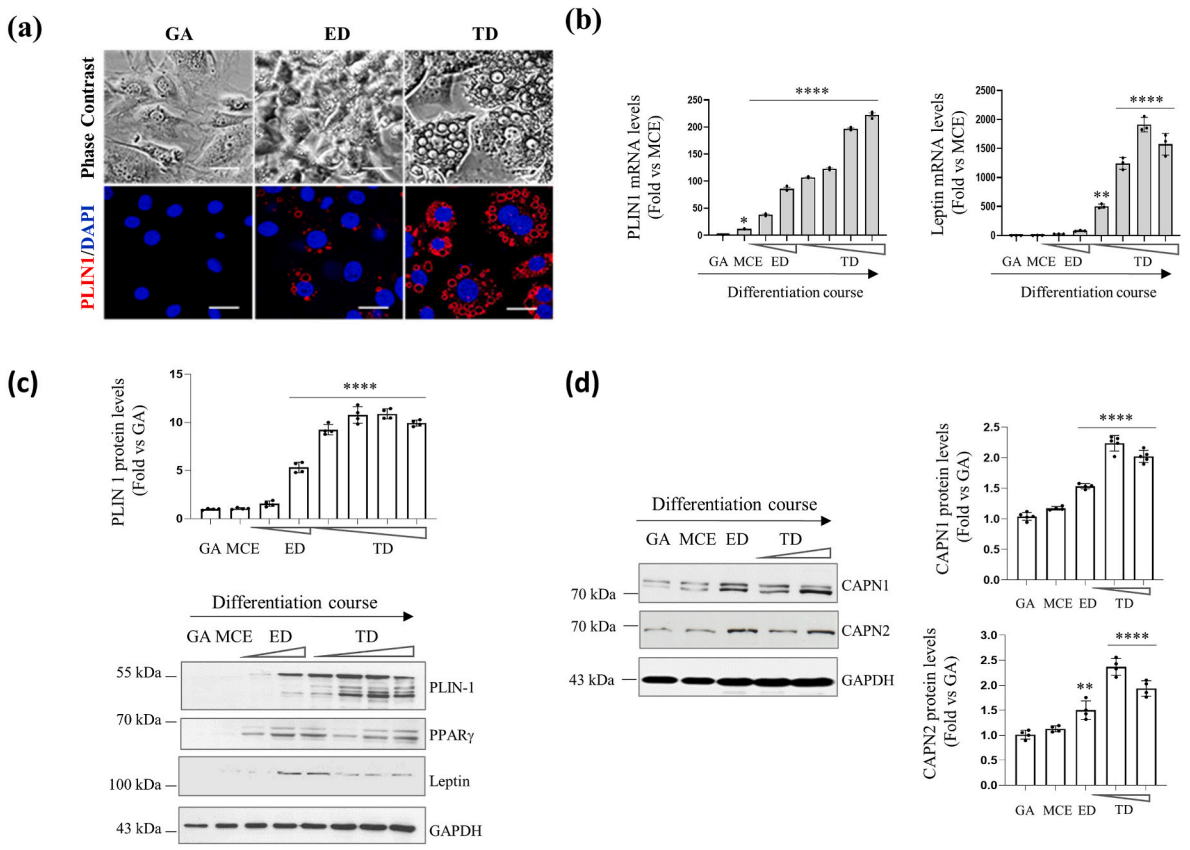

Fig. 1. Phase-specific abundance of CAPNs during MDIR-induced preadipocyte differentiation. (a) Phase contrast (upper panels) and perilipin-1 (red) immunofluorescent staining (lower panels) of 3T3-L1 cells at GA, ED and TD stages after MDIR-induced differentiation. Nuclei were stained with DAPI (blue). Scale bars, 21 μm. Representative images ($n \geq 3$) of phase contrast and confocal microscopy are shown. (b) Perilipin-1 (left) and Leptin (right) mRNA levels analysed by RT-qPCR along 3T3-L1 induced-differentiation. Data were normalized by 18S, quantified and plotted as fold vs. GA. Results ($n \geq 3$) are means ± SD. (c) Total protein levels of PLIN-1, PPARγ, Leptin and GAPDH were analysed by Western blot during the time course of differentiation. Perilipin-1 protein levels were quantified, normalized with GAPDH and plotted as the mean fold ($n \geq 3$) ± SD vs. GA. (d) Analysis of CAPN1 (upper) and CAPN2 (lower) protein levels along the 3T3-L1 differentiation course. Protein levels were quantified, normalized with GAPDH and plotted as the mean fold ($n \geq 3$) ± SD vs. GA. Statistical significance was: *$p < 0.05$, **$p < 0.01$ and ****$p < 0.0001$ vs GA.

anchor helix relieves structural constraints permitting realignment of the catalytic triad and formation of the catalytic cleft essential for activation. This indirect evidence of calpain activation was analysed by Western blot as means of Nt/Ct-CAPN1 ratio, using an antibody specific to Nt-CAPN1 or Ct-CAPN1 (Fig. 2A). The Nt/Ct-CAPN1 ratio showed a significant decline at the MCE stage and thereafter, suggesting an early activation of CAPN1 during 3T3-L1 differentiation.

Cleavage and dissociation of the small regulatory subunit CAPNS1 have been linked to high calpain activity [7,24]. According to the upregulation of both catalytic subunits, CAPNS1 levels progressively increased throughout differentiation (Fig. 2B). However, CAPNS1 proteolysis was not detected. On the other hand, CAST, the endogenous inhibitor of both calpain isoforms, was absent at early stages of differentiation but showed a marked increase during the ED-TD transition and at the TD stage (Fig. 2B). CAST levels are expected to increase after calpains upregulation to limit an excessive calpain activity [25]. Increased CAST levels suggest that its inhibitory activity may be required at later stages to prevent excessive calpain activation. Indeed, increased calpain activity during adipocyte differentiation was confirmed by enzymatic assay (Fig. 2C). These findings indicate that both, CAPN levels and activity are upregulated at the end of MCE and the onset of ED.

3.3. Subcellular distribution of calpains during 3T3-L1 differentiation

Calpains seem to be key enzymes during the MCE-to-ED transition in hormonally-induced differentiation of 3T3-L1 cells. However, since 3T3-L1 differentiation is a sequential process, the particular contribution of each isoform to a specific stage remains unclear. The subcellular distribution of isoform-specific calpains is crucial for substrate recognition and functions [10,12,26,27]. Consequently, the subcellular localization of CAPN1 during MDIR-induced differentiation of 3T3-L1 cells was examined by IF staining. PLIN-1 co-immunostaining was used to accurately correlate CAPN1 distribution with the differentiation stages.

CAPN1 was significantly redistributed throughout the differentiation process (Fig. 3A). In fibroblast-shaped GA pre-adipocytes, CAPN1 was diffusely localized in both the nucleus and cytoplasm. During MCE, some cells displayed pronounced CAPN1 aggregates within the nucleus (Fig. 3B), which persisted through ED and were reorganized in nucleoli during ED-TD transition. Once differentiation was completed, CAPN1, not detected in nuclear aggregates, was predominantly found in the cytosol, close to cell membranes and lipid droplets.

Western blot analysis of subcellular fractions confirmed CAPN1 distribution during pre-adipocyte differentiation (Fig. 3C). Consistent with the IF data, nuclear CAPN1 was firstly detected during MCE-ED transition, persisted during ED-TD and declined upon the completion of differentiation.

Interestingly, CAPN2 was differentially distributed over the same time-course of adipocyte differentiation (Fig. 4A). This isoform was primarily found in the cytoplasm throughout the differentiation process and did not form nuclear aggregates. However, a minor fraction of CAPN2 also translocated to the nuclei of adipocytes during ED as a

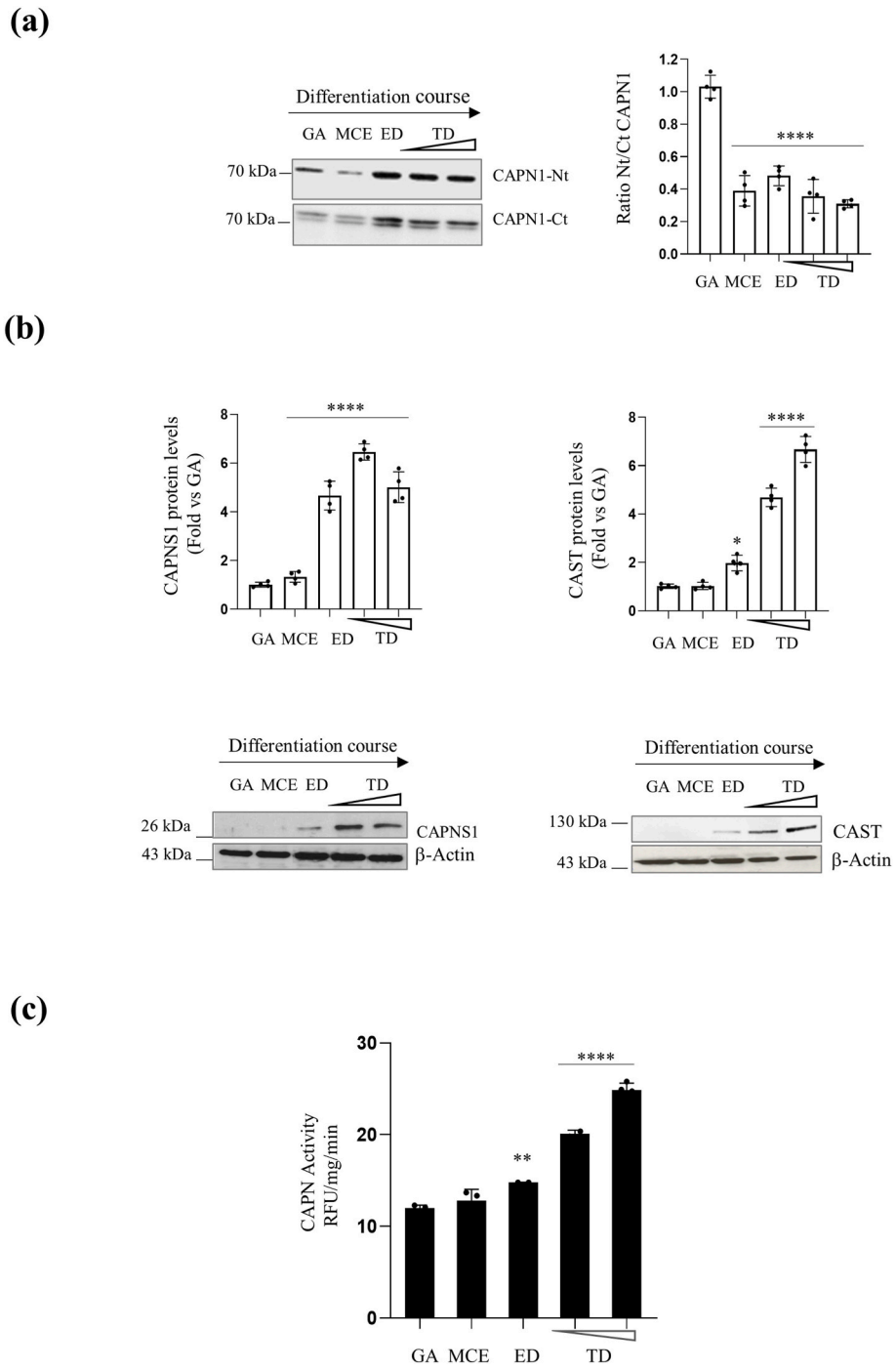

Fig. 2. Calpain-calpastatin axis during the time-course of 3T3-L1 differentiation. Total protein samples from MDIR-induced 3T3-L1 adipocytes were analysed at GA, MCE, ED and TD stages. Representative images are shown. (a) Nt-CAPN1 and Ct-CAPN1 protein levels analysed by Western blot with α-Ct-CAPN1 or α-Nt-CAPN1 specific antibodies, were quantified and plotted as the ratio Nt-CAPN1/Ct-CAPN1. Protein levels of (b) CAPNS1 (left) and CAST (right) were quantified, normalized with β-actin and plotted as mean fold ($n \geq 3$) ± SD vs. GA. (c) Calpain activity at different stages of adipocyte differentiation. Statistical differences were $^{**}p < 0.01$ and $^{****}p < 0.0001$vs GA.

nuclear punctuate and remained there until the TD stage (Fig. 4B). CAPN2 was relocalized to the cytosol in fully differentiated adipocytes.

Subcellular distribution, as analysed by Western blot (Fig. 4C), indicated that while cytoplasmic CAPN2 levels remained relatively high and steady throughout the entire differentiation process, nuclear CAPN2 levels, initially low, increased at MCE and remained constant until the end of TD.

These results demonstrate that both calpains undergo significant nuclear relocalization at the MCE stage. Moreover, our findings suggest that nuclear CAPN1 aggregates might be related to interphase rather than to mitosis. Although we unknow the nature of these nuclear aggregates, apparently the same punctate-stained regions were previously identified in 3T3-L1 cells as nuclear sites of DAPI fluorescence, known to strongly interact with centromeric heterochromatin at the S phase entrance [28]. The distinct subnuclear localization of CAPN1 and CAPN2 during pre-adipocytes differentiation reinforce the hypothesis of the isoform-specific functions of calpains during this process.

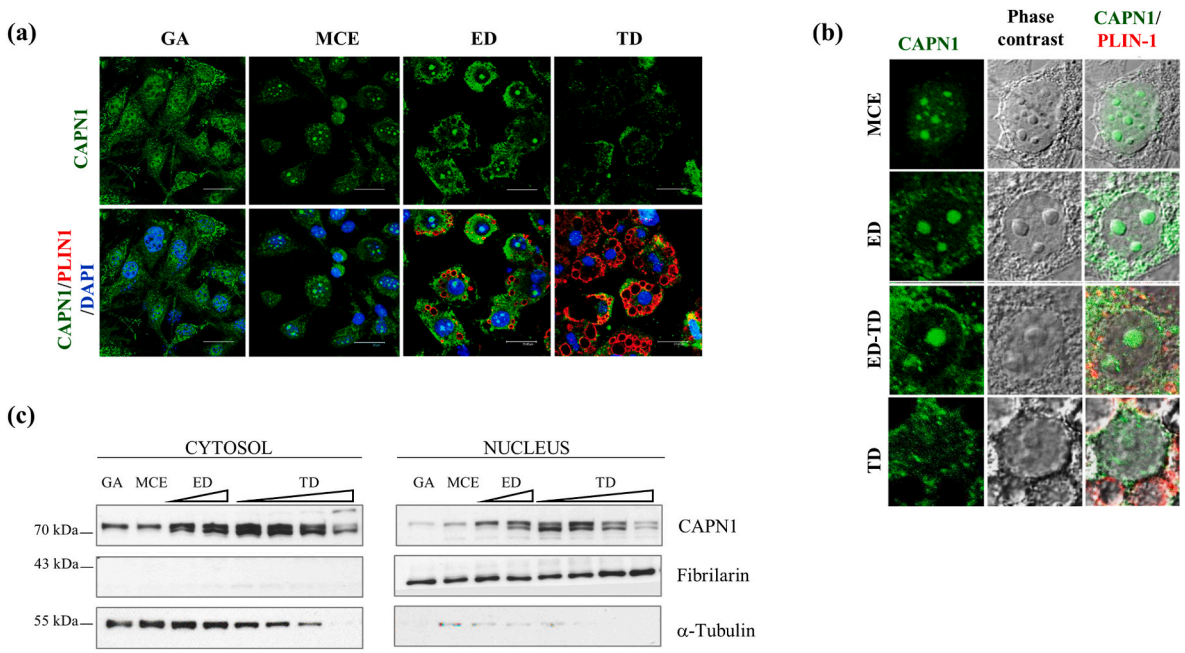

Fig. 3. Phase-dependent subcellular localization of CAPN1 during preadipocyte induced-differentiation. (a) Immunostaining of CAPN1 (green) and perilipin-1 (red) in 3T3-L1 cells during GA, MCE, ED and TD stages. Nuclei were stained with DAPI (blue). Scale bar, 21 μm. Representative images are shown (n ≥ 3). (b) Detailed subcellular localization of CAPN1 in 3T3-L1 single cells along the differentiation course. Immunofluorescence staining and phase contrast images are shown (c) Changes in CAPN1 levels along 3T3-L1 differentiation course were analysed in cytosolic and nuclear fractions by Western blot. Fibrillarin and α-tubulin were used as markers of fraction purity. Equal loading was assessed by Ponceau-staining of membranes.

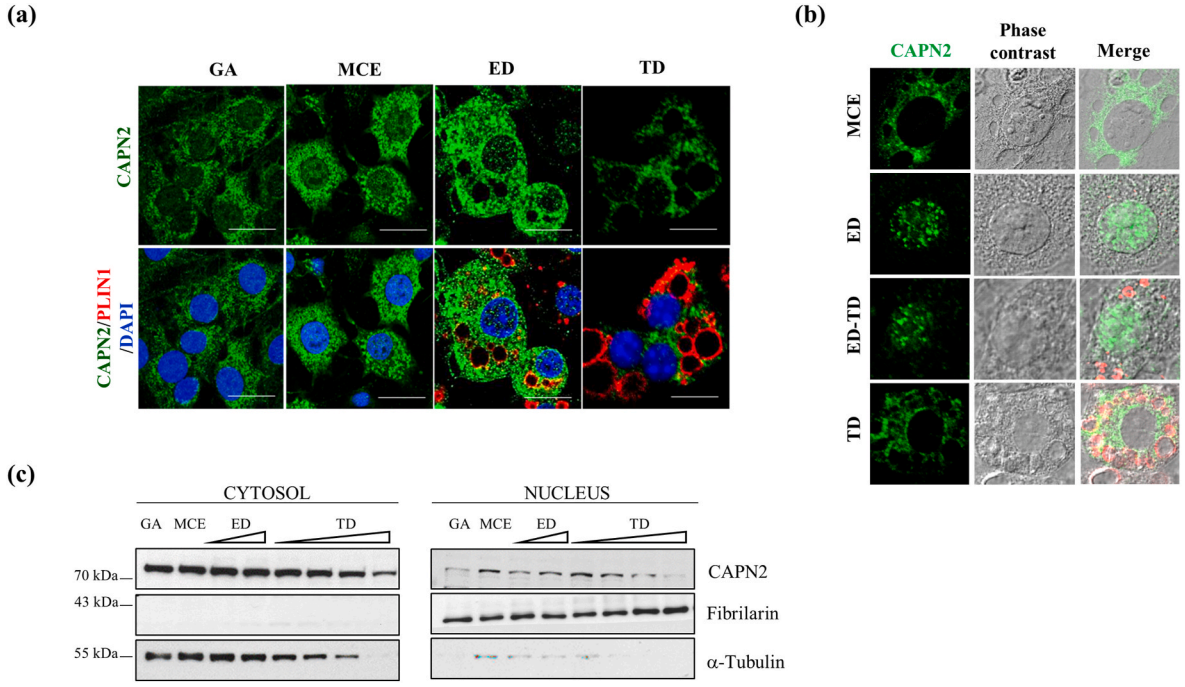

Fig. 4. Subcellular distribution of CAPN2 along preadipocyte induced-differentiation. (a) Immunostaining of CAPN2 (green) and perilipin-1 (red) in 3T3-L1 cells at GA, MCE, ED and TD phases. Nuclei were stained with DAPI (blue). Scale bar, 21 μm. Representative images are shown (n ≥ 3). (b) Detailed subcellular localization of CAPN2 in 3T3-L1 single cells along the differentiation course. Immunofluorescence staining and phase contrast images are shown (c) Changes in CAPN2 levels along 3T3-L1 differentiation course were analysed in cytosolic and nuclear fractions by Western blot. Fibrillarin and α-tubulin were analysed as markers of fraction purity. Equal loading was assessed by Ponceau-staining of membranes.

3.4. Functional role of CAPNs during pre-adipocyte differentiation at MCE-ED

As already mentioned, general inhibitors of cys-proteases such as ALLN have been reported to inhibit 3T3-L1 differentiation by blocking their entrance into MCE. The same results were obtained in CAST overexpressing cells [6,13,14]. However, the isoform-specific role of calpains in this process remains unknown. To study the function of both

isoforms during MCE and ED, CAPN1 or CAPN2 were knocked-down in 3T3-L1 48 h before MDIR-induction and the effect analysed at specific stages. As shown in Fig. 5A, at MCE-ED transition both CAPNs were efficiently depleted. Although not completely blocked, lower oil Red staining of lipid droplets in siCAPN1 and siCAPN2 transfected cells (Fig. 5B) suggests that both calpains might be modulating MCE-ED transition. We investigated whether MCE-ED transition was delayed or prevented by CAPNs silencing. Upregulation of C/EBPα mRNA levels is known to occur at late MCE when cells exit the cell cycle. In fact, C/EBPα is thought to be responsible for terminating mitotic clonal expansion [29]. C/EBPα mRNA levels in siCAPN1 and siCAPN2-transfected cells were strongly down-regulated during MCE-ED transition (Fig. 5C). It has been suggested that once MCE-ED transition is blocked, differentiation of 3T3-L1 cannot be completed [17]. mRNA levels of the TD marker Leptin, were also down-regulated in siCAPN1 and siCAPN2 depleted cells (Fig. 5C), indicating that the differentiation program was partially prevented. Accordingly, our data might indicate that both calpains are involved in the pre-adipocytes exit from S phase and termination of MCE.

The percentage of cells at each phase of cell cycle during MCE was analysed in scRNA and siCAPN1 or siCAPN2-transfected cells. The number of cells at S phase after CAPN-depletion was two-fold higher than in control cells (Fig. 5D). Interestingly, the same percentage of cells at the S phase was found after depletion of either CAPN1 or CAPN2. Increased levels of p53 lead to cell cycle arrest at S phase [30]. Higher levels of p53 were also observed in siCAPN1 and siCAPN2 transfected cells (Fig. 5E). Consequently, these data suggest that both calpains modulate MCE at the S phase. Moreover, rather than at MCE entrance as previously suggested [14], the role of calpains seems to be at the MCE exit.

3.5. Nuclear function of calpains on the epigenetic program of 3T3-L1 differentiation

During adipogenic differentiation, changes of chromatin interactions, structure and positioning at the MCE stage are usually accompanied by changes in gene expression. These changes are thought to be part of the priming events essential for the MCE-ED transition [31]. As shown in Fig. 3, DAPI staining during MCE shows a punctate pattern, which has been previously identified as interaction sites between DAPI and heterochromatin in mouse chromosomes [32]. A similar punctuate pattern was obtained with CAPN1 staining. Our previous work demonstrated the CAPN1-mediated proteolysis of histone H3 in adipocyte-enriched fractions from post-lactation mammary tissue [27]. Although in the current experiments the punctuate sites of CAPN1 and DAPI colocalization were not identified as heterochromatin, we hypothesize that the CAPN1-mediated clipping of H3 could play a role in the priming events during pre-adipocyte MCE.

Histone H3 from MDIR-stimulated pre-adipocytes showed faster migrating bands when immunodetected with antibodies recognizing the C-terminal region. Truncated histone H3 was detected at ED-TD transition and in fully differentiated adipocytes (Fig. 6A). CAPN1-mediated proteolysis of histone H3 was confirmed by *in vitro* experiments with adipocyte extracts and recombinant histone H3 (Supplementary Fig. S8). Additionally, to exclude that H3 proteolysis could be the consequence of sample manipulation [33], cells were treated with either calpeptin or ALLN prior to MDIR induction. Calpain activity was efficiently inhibited by both, ALLN and calpeptin (Supplementary Fig. S9). Inhibition of calpain activity partially prevented 3T3-L1 differentiation as shown by oil red staining (Fig. 6B), PLIN-1 protein levels (Fig. 6C) or C/EBPα expression (Fig. 6D) at ED. Moreover, the expression of leptin, the molecular marker of the TD stage was also partially prevented by calpeptin (Fig. 6D). Histone H3 was analysed in calpeptin and ALLN-treated cells at the TD stage, when enough cleaved H3 was accumulated to be detected. Proteolytic cleavage of Nt-H3 tail was fully prevented by both inhibitors (Fig. 6E). Although all these findings support the hypothesis of calpain-mediated cleavage of Nt-H3 tails, the cleavage product was not detected at earlier stages during the MCE-ED transition. Consequently, evidences for the calpain-mediated cleavage of H3 at earlier stages of 3T3-L1 differentiation should be obtained.

Cleavage of histone H3 during GA, MCE and ED was further analysed in 3T3-L1 by IF detection of overlapping/non-overlapping staining of both, Ct-H3 and Nt-H3 (Fig. 6F). The Ct-H3 and Nt-H3 signals overlapped at the GA stage and in fully differentiated adipocytes (TD). However, no overlapping was observed during MCE and ED. The calpain-mediated cleavage of histone H3 was most likely initiated at MCE, although only at later stages truncated histone H3 can be detected by Western blot.

To confirm this hypothesis a direct *in vivo* interaction between calpains and histone H3 was investigated at MCE and ED-TD transition by the sensitive in situ Duolink PLA. In these assays, a fluorescent signal is generated only when the plus and minus probes attached to each antibody are bound together. As shown in Fig. 7A, PLA assay revealed a direct interaction between CAPN1 and the Nt-H3 tail at the MCE stage in MDIR-induced 3T3-L1 cells. Conversely, no interaction at all was detected at ED-TD transition suggesting that the Nt-H3 tails had already been cleaved or that calpains were no longer interacting with histone H3 at this stage. A much weaker, interaction pattern was observed for CAPN2 and Nt-H3. Quantification of PLA signal per nucleus indicated that CAPN2/Nt-H3 interactions at the MCE were negligible compared to CAPN1/Nt-H3 interactions (Fig. 7B).

Accordingly, histone H3 cleavage analysed at the TD (Fig. 7C) was prevented by CAPN1 depletion. These data indicate that CAPN1 is most likely the isoform mainly contributing to this epigenetic mark during MCE of differentiating 3T3-L1 preadipocytes.

4. Discussion

Adipose tissue is a dynamic organ crucial for maintaining energy balance, homeostasis, and body weight control. A key factor in adipose tissue dysfunction is the inability of adipose precursor cells to generate new adipocytes, highlighting the importance of this process in preserving tissue health and functionality. Here, we provide evidence demonstrating that both, calpain-1 and calpain-2 contribute to 3T3-L1 pre-adipocyte differentiation, as evidenced by their increased expression and activity during the process.

Other reports have demonstrated that calpain activity is involved in the modulation of the differentiation of adipocytes or even other cell types such as neural and mesenchymal stem cells, chondrocytes and osteoblasts [6]. However, most of these were only supported by the observation that inhibition of calpain activity by ALLN also inhibits cell differentiation. Yet, ALLN widely used to inhibit calpain activity, can also inhibit other proteases such as cathepsins, neutral cysteine proteases or the proteasome [5]. In other reports CAST was overexpressed to inhibit calpains during adipocyte differentiation but, since CAST can inhibit different calpains, the specific contribution of each calpain isoform is still missing [6,13,14,16]. Instead, we used calpeptin, a recognized specific chemical inhibitor of calpain activity, or calpains silencing by siRNA transfection to demonstrate the calpain-mediated differentiation of 3T3-L1 pre-adipocytes. Indeed, our analysis in calpeptin pre-treated cells or in cells transfected with siCAPN1 and siCAPN2 prior to MDIR-stimulation, showed decreased Plin-1, C/EBPα and leptin levels, supporting the adipogenic function of calpains during the early events of 3T3-L1 differentiation.

In contrast to our data, it has been reported that while CAPN2 and CAST protein levels increase, the expression of CAPN1 is down-regulated in hormonally stimulated 3T3-L1 or ST-13 cells [6,13,34]. Moreover, it was suggested that calpain is an inducer of adipogenesis in 3T3-L1 cells, but a repressor of adipogenesis in ST-13 cells [6,16]. Although a model-dependent effect of calpains on adipocyte differentiation cannot be ruled out, discrepancies are most probably caused either by some conclusions based on the use of non-specific inhibitors of

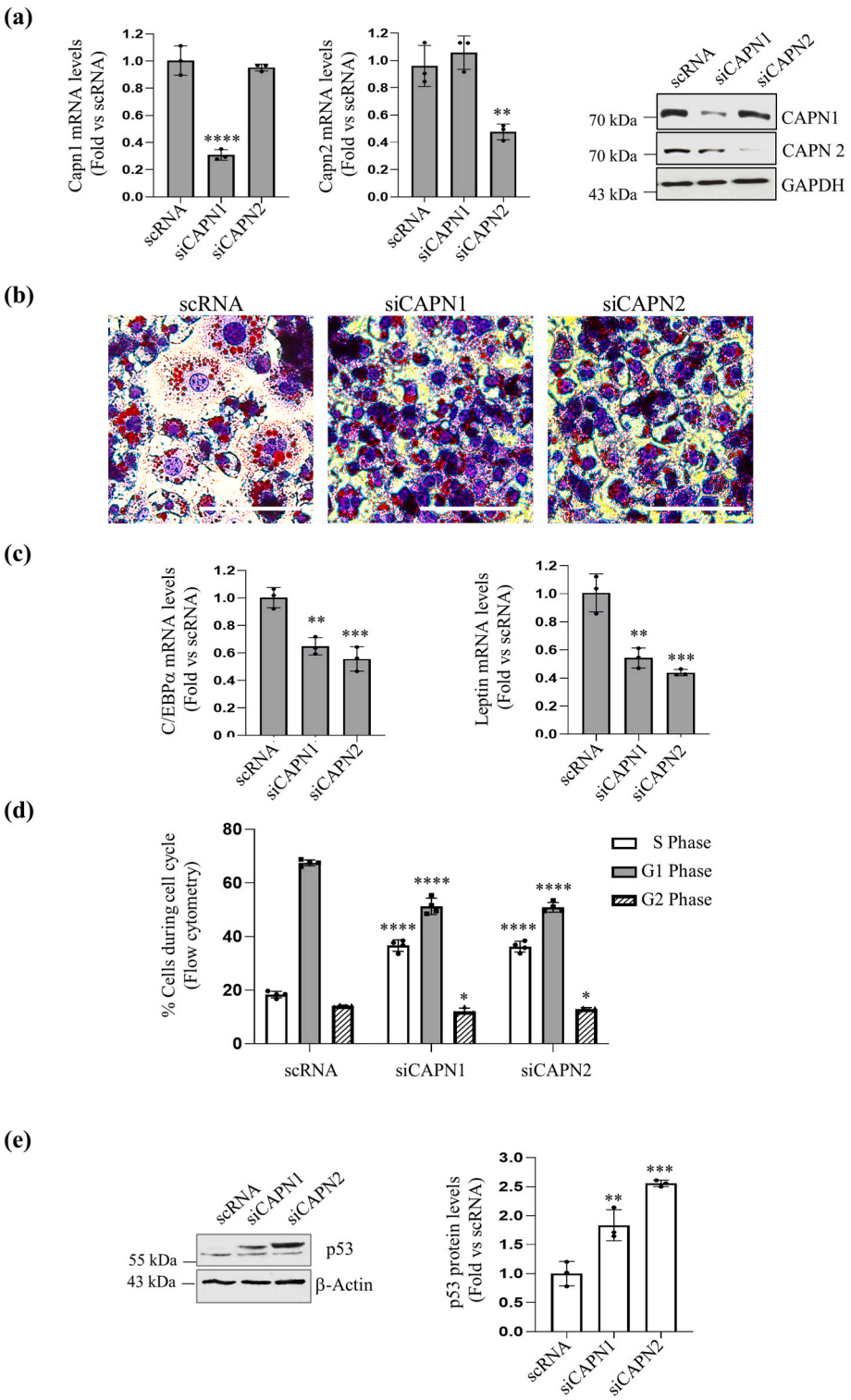

Fig. 5. Effect of calpains depletion on MCE-to-ED transition of hormonally-stimulated 3T3-L1 cells. Cells were transfected with scRNA, siCAPN1 or scCAPN2 48 h prior to MDIR induction of differentiation (a) Knock-down efficiency was analysed by RT-qPCR (left) and Western blot (right) at MCE-ED phase in scRNA, siCAPN1 and siCAPN2-transfected 3T3-L1 cells. (b) Oil Red O staining of triglycerides and lipids (red) in scRNA, siCAPN1 and siCAPN2-transfected 3T3-L1 cells at MCE-ED stage. Nuclei were counterstained in blue. Representative images are shown (n ≥ 3). Scale bar, 100 μm. (c) C/EBPα mRNA levels at MCE-ED (left) and Leptin mRNA levels at ED-TD (right) were analysed by RT-qPCR in scRNA, siCAPN1 and siCAPN2-transfected 3T3-L1 cells. Data were quantified, normalized according to 18S and plotted as mean (n ≥ 3) fold ± SD. (e) Percentage of cells at cell cycle phases in scRNA, siCAPN1 and siCAPN2-transfected cells analysed by flow cytometry at MCE-ED. Values were plotted as mean (n = 3) fold ± SD vs. scRNA transfected-cells (f) Total protein levels of p53 were analysed by Western blot in scRNA, siCAPN1 and siCAPN2-transfected 3T3-L1 cells during MCE-ED. Protein levels were quantified, normalized by β-actin levels and plotted as mean (n = 3) fold ± SD vs. scRNA. Statistical significances were: *p < 0.05, **p < 0.01, ***p ≤ 0.001, and ****p ≤ 0.0001 vs scRNA transfected cells.

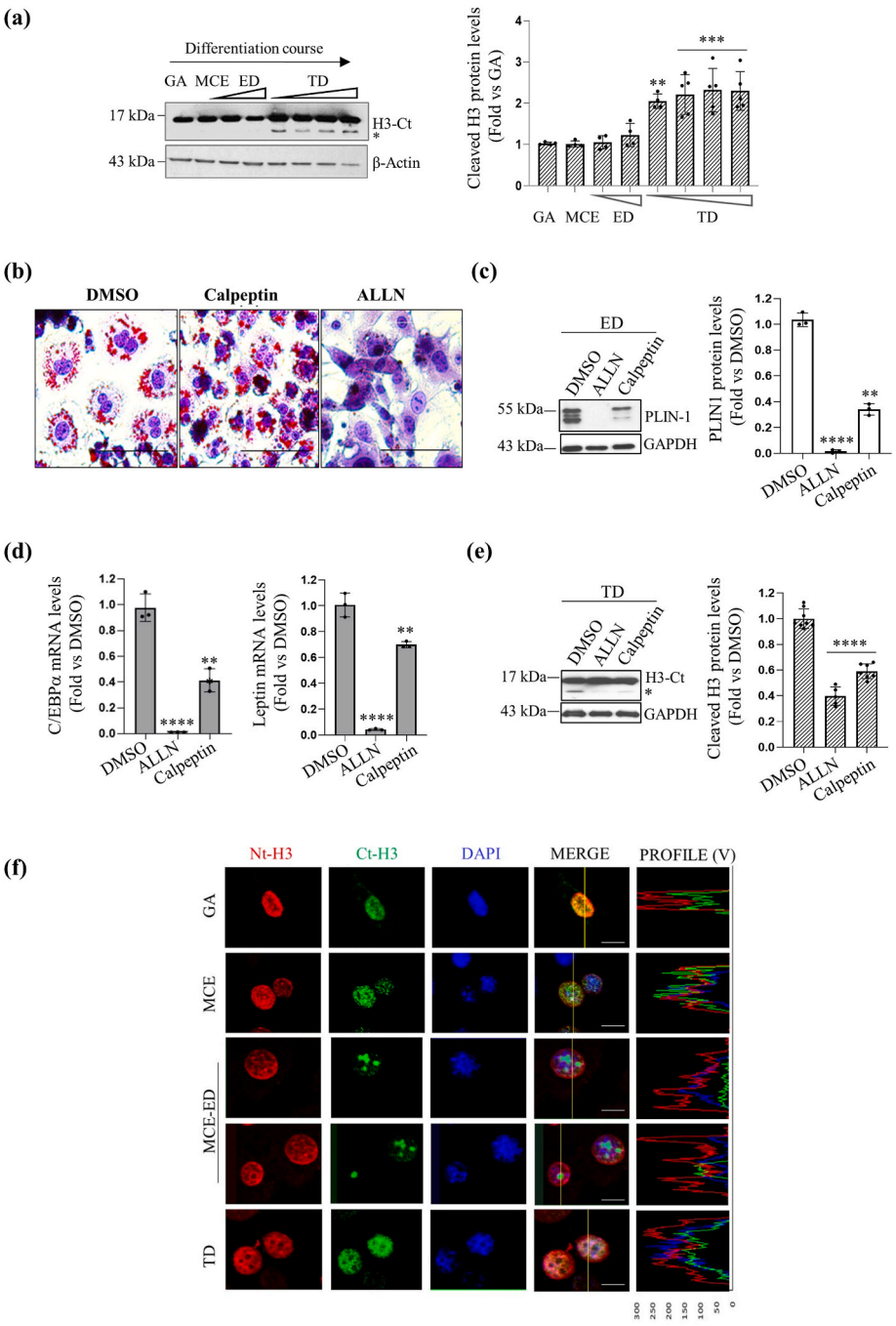

Fig. 6. Role of calpain activity on the cleavage of histone H3 N-terminal tails. (a) Western blot analysis of histone H3 N-tail cleavage with an antibody recognizing the C-terminal end of histone H3. Full length and (*) truncated histone H3 protein levels were quantified, normalized with GAPDH and plotted as the mean fold ($n \geq 3$) ± SD vs GA. (b) 3T3-L1 cells were pre-treated with DMSO, calpeptin or ALLN before MDIR-induction and analysed at MCE-ED by Oil Red O staining. Representative images are shown ($n \geq 3$). Scale bars, 100 μm. (c) Perilipin-1 protein levels were quantified, normalized with GAPDH and plotted as the mean fold ($n \geq 3$) ± SD vs DMSO. (d) C/EBPα at MCE-ED transition (right) and leptin at ED-TD (left) mRNA levels were analysed by RT-qPCR. Data were normalized by 18S and plotted as mean fold ± SD vs DMSO ($n \geq 3$). (e) Cleavage of the N-terminal tail of histone H3 in total protein extracts from DMSO, calpeptin and ALLN-pretreated 3T3-L1 cells was analysed at TD by Western blot. GAPDH was used as loading control and cleaved H3 products were quantified and plotted vs DMSO. (f) Immunofluorescence staining of N-terminal (red) and C-terminal (green) histone H3 ends in GA, MCE, MCE-ED and TD stages of 3T3-L1 differentiation. Nuclei were counterstained with DAPI (blue). Merge images and their vertical profiles are shown in right panels. Representative images are shown ($n \geq 3$). Scale bars are 10 μm. For bar graphs statistical significances were: $^{**}p < 0.01$, $^{***}p \leq 0.001$, and $^{****}p \leq 0.0001$.

calpain activity, or by differences in the experimental design such as: (i) Rosiglitazone not included in the stimulation cocktail to induce differentiation; (ii) Preadipocytes not arrested at the GA state when stimulated (critical for this dynamic model) [20,21]; (iii) Dominant negative calpain or CAST overexpressed before cells reached the GA stage; (iv) Cells were treated with inhibitors or ionophores at ED-TD transition [16]; (v) Finally, the absence of a comprehensive analysis of subcellular and subnuclear distribution, the study of the complete calpain/calpastatin axis and/or the indirect analysis of changes in calpain activity throughout the time-course of differentiation. Herein, we carefully correlated the pattern of morphological and molecular changes during differentiation with calpain levels. In addition, our data indicate that not

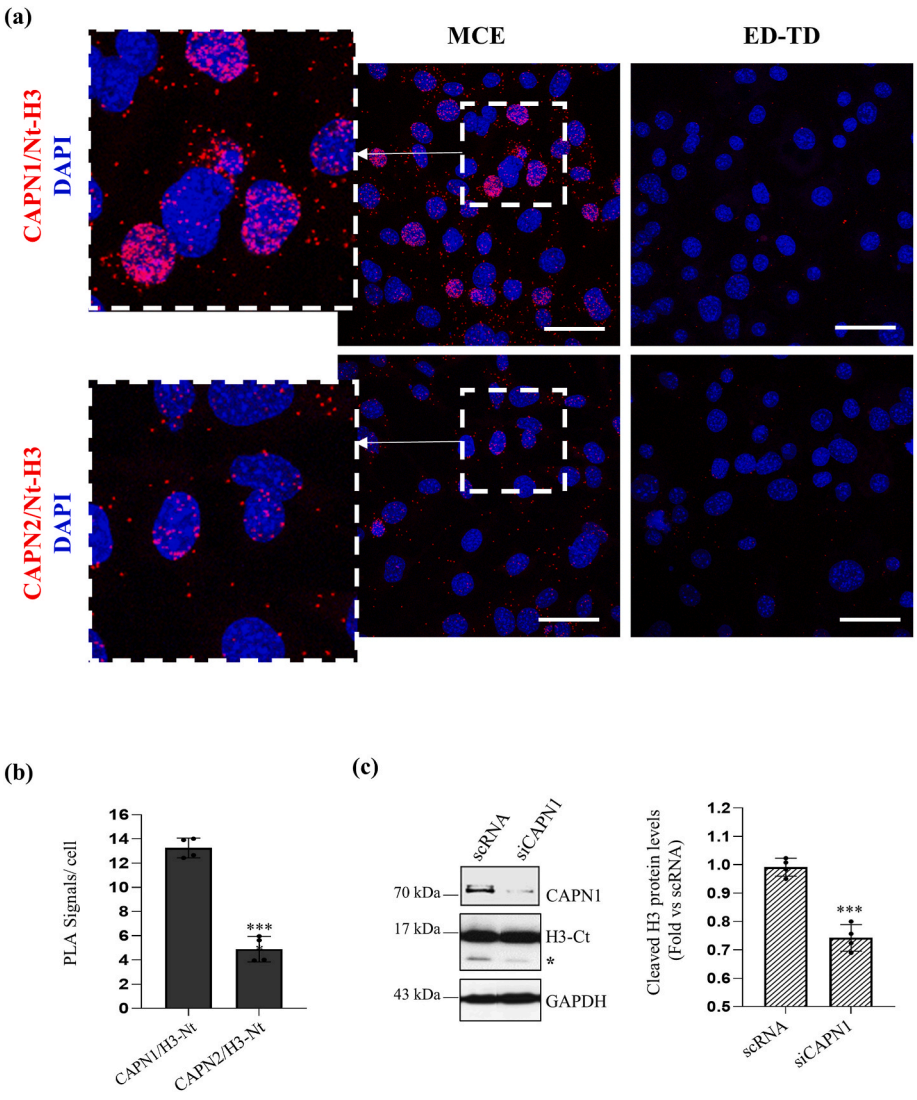

Fig. 7. Calpain-mediated cleavage of N-terminal tails of Histone H3 during MCE. (a) CAPN1/histone H3-Nt (upper panel) and CAPN2/histone H3-Nt (lower panel) interaction was analysed by PLA assay in 3T3-L1 cells during MCE and ED-TD differentiation phases (red spots). Nuclei were stained with DAPI (blue). Representative images are shown ($n \geq 3$). Scale bar, 21 μm. (b) Quantification of PLA signals obtained from CAPN1/H3-Nt and CAPN2/H3-Nt interactions as the number of PLA signals/cell. (c) Cleavage of histone H3 was analysed in scRNA and siCAPN1-transfected cells at TD phase with an antibody directed towards histone H3-Ct. Blots show full and truncated(*) H3. Protein levels of CAPN1 were also analysed to demonstrate knocking down efficiency. Truncated histone H3 levels were quantified, normalized by GAPDH and plotted as mean fold ($n \geq 3$) ± SD, ***$p < 0.001$, vs scRNA.

only the expression, but also CAPN activity was upregulated during MCE, as evidenced by the decrease of Nt/Ct-CAPN1 ratio at this stage, increased and the later accumulation of CAST protein levels at TD and increased enzymatic activity.

In agreement with previous reports, the role of calpains seems to be crucial for the MCE triggered by MDRI-stimulation. Inhibition of calpain activity or depletion of calpains in siCAPN1 and siCAPN2-transfected cells after the MCE stage, did not inhibit full differentiation of 3T3-L1 cells (data not shown). Many studies on the mechanisms of the differentiation program are focused on early key factors triggering MCE-ED transition such as, PPARγ and C/EBPα; In fact, abrogation of PPARγ or C/EBPα upregulation is known to block full differentiation of adipocytes. However, although identified as key factors for adipocyte differentiation, none of them are upregulated during the first phases of preadipocyte differentiation [1]. Actually, expression of C/EBPα indicates MCE termination [29]. Moreover, as already mentioned, it seems that MCE is not needed for full differentiation of non-embryonic adipocytes [16]. Accordingly, a role for CAPN activity at earlier time points after MDRI-induced differentiation of 3T3-L1 cells should not be ruled out. The approaches followed in our experiments would not allow the detection of a low but functionally significant increase of CAPN activity soon after MDIR-treatment before the entrance into MCE. However, we observed that during MCE, calpain-depleted cells were accumulated at S phase 24 h after MDIR stimulation, when cells are supposed to express C/EBPα and exit MCE [29]. Accordingly, the increased number of calpain-depleted cells at S phase indicate that rather than controlling the entrance as previously suggested [14] calpains are most likely modulating the exit from the MCE stage. In agreement with this, p53 tumour suppressor known to induce S-phase arrest, was significantly increased in calpain knock-down cells. It is noteworthy to mention that p53 is one of the first calpain-targets to be identified [35] and one of the most recognized modulators of adipocyte differentiation [30]. While ectopic expression of p53 during MCE inhibits adipocyte differentiation, depletion of p53 in knockdown cells enhances their adipogenic capacity [30].

On the whole, our data demonstrate that calpains expression and subcellular distribution follow a phase-specific pattern during the differentiation of 3T3-L1 preadipocytes, suggesting that these proteases are

involved in the control of particular stages. Expression analysis of MDIR-treated 3T3-L1 cells showed that both, CAPN1 and CAPN2 are upregulated after stimulation, progressively increase during the ED-TD transition and subsequently decreased upon the completion of differentiation, highlighting their temporal involvement in this process. Translocation of both calpains to the cell nucleus also follows a stage-specific pattern. The different subnuclear distribution of CAPN1 (nuclear aggregates signal) and CAPN2 (diffuse nucleoplasmic signal) is likely to restrict their interaction with substrates, ultimate leading to different functional consequences. In addition, CAPN1 nuclear translocation seems to begin earlier (MCE) than CAPN2, which rises during the MCE-ED transition.

Other studies on the mechanisms underlying the function of nuclear calpain in adipocyte differentiation were also focused on the MCE stage. However, early reports attempt to explain calpain functions as the result of cleaving key proteins involved in adipogenic differentiation, including transcription factors or cell cycle inhibitors [6,13,14,16,34,36]. Although not completely understood, an increasing number of reports propose that adipogenesis is governed by a complex epigenetic program. Rather than focusing solely on key differentiation factors, these studies emphasize the importance of epigenetic marks on adipogenic genes, which are thought to initiate a cascade of sequential events [37]. Few hours after MDIR-treatment, pre-adipocytes suffer important changes in the nuclear compartment that affect adipogenic genes such as, relocation of gene positioning, interactions between adipogenic gene promoters previous to their transcription, and chromatin remodelling [4,31,37,38].

Calpains might take part in such epigenetic program through the modification of histone H3. The proteolytic cleavage of Nt-H3 tails have been previously described during the differentiation of several cell types and by different proteases [38]. We previously reported the CAPN1-dependent cleavage of Nt-H3 in adipose fractions from mammary gland after lactation [27]. However, we could not show at that time the *in vivo* interaction between CAPN1 and H3. Herein, the direct interaction of CAPN1 with the Nt-H3 in adipocytes at the MCE stage was demonstrated by the sensitive PLA technique. Interestingly, once Nt-H3 was cleaved, no PLA or Nt/Ct-H3 overlapping IF signal was detected at ED-TD. We could hypothesize that histone clipping is needed for the expression of adipogenic genes and MCE-ED transition.

All in all, we were not able to completely dissect the role of both calpains during 3T3-L1 differentiation. In all our experiments disruption of CAPN-1 or CAPN-2 expression has apparently the same functional antiadipogenic effect. Complementary functions for calpain-1 and -2 in other processes has been already described [10,39,40]. While calpain-1 modulates the initial steps of synaptic plasticity, calpain-2 activation restricts the extent of plasticity [10]. Our data also lead to hypothesize that the complementary functions of both calpains modulate the MCE-ED transition. It has been recently suggested that multiple proteases can target H3 in the same context, providing a new perspective for the role of cys-proteases, ser-proteases and metalloproteases known to cleave Nt-H3 tails during cell differentiation [4]. CAPN2 might also contribute to histone H3 cleavage, even though its interaction with H3 at the MCE stage was minimal compared to the CAPN1.

5. Conclusions

In summary, our findings highlight that CAPN1 and CAPN2 play phase-specific functions in the differentiation of 3T3-L1 preadipocytes. Both calpains exhibit dynamic expression patterns and distinct subnuclear localizations, contributing to the regulation of MCE and the subsequent stages of differentiation. CAPN1 involvement in histone H3 modification suggests a potential role in the epigenetic programming of adipogenesis.

Future studies should explore the interplay between calpains and other proteases that contribute to a precise pattern of histone modifications crucial for cellular differentiation, as well as identify those calpain substrates mediating their functions during adipogenesis. Understanding these mechanisms could provide new insights into adipose tissue biology and unveil novel therapeutic targets for obesity and metabolic disorders.

CRediT authorship contribution statement

L. Rodríguez-Fernández: Writing – review & editing, Validation, Methodology, Investigation, Formal analysis, Data curation. **R. Zaragozá:** Writing – review & editing, Visualization, Validation, Supervision, Formal analysis, Data curation, Conceptualization. **J.R. Viña:** Writing – review & editing, Project administration, Funding acquisition. **E.R. García-Trevijano:** Writing – review & editing, Writing – original draft, Visualization, Validation, Supervision, Project administration, Investigation, Funding acquisition, Formal analysis, Conceptualization.

Disclosure statement

Authors declare no potential conflict of interest.

Funding

This research was supported by the Generalitat Valenciana. Conselleria d'Educació, Investigació, Cultura i Esport [grant number GVPROMETEO CIPROM/2021/051 (to ERG-T and JRV)].

Acknowledgments

We acknowledge the contribution of our Master degree and PHD students and all the laboratory members to the research in the field of calpains.

Appendix A. Supplementary data

Supplementary data to this article can be found online at https://doi.org/10.1016/j.abb.2025.110557.

Data availability

No data was used for the research described in the article.

References

[1] Y.-Y. Mo, et al., Adipose tissue plasticity: a comprehensive definition and multidimensional insight, Biomolecules 14 (10) (Sep. 2024) 1223, https://doi.org/10.3390/biom14101223.
[2] M. Zamboni, et al., Adipose tissue, diet and aging, Mech. Ageing Dev. 136–137 (Mar. 2014) 129–137, https://doi.org/10.1016/j.mad.2013.11.008.
[3] G. Colleluori, J. Perugini, G. Barbatelli, S. Cinti, Mammary gland adipocytes in lactation cycle, obesity and breast cancer, Rev. Endocr. Metab. Disord. 22 (2) (Jun. 2021) 241–255, https://doi.org/10.1007/s11154-021-09633-5.
[4] K.J. Ferrari, et al., Intestinal differentiation involves cleavage of histone H3 N-terminal tails by multiple proteases, Nucleic Acids Res. 49 (2) (Jan. 2021) 791–804, https://doi.org/10.1093/nar/gkaa1228.
[5] Y. Xiao, et al., Cathepsin K in adipocyte differentiation and its potential role in the pathogenesis of obesity, J. Clin. Endocrinol. Metab. 91 (11) (Nov. 2006) 4520–4527, https://doi.org/10.1210/jc.2005-2486.
[6] Y. Yajima, S. Kawashima, Calpain function in the differentiation of mesenchymal stem cells, Biol. Chem. 383 (5) (May 2002) 757–764, https://doi.org/10.1515/BC.2002.079.
[7] R.L. Campbell, P.L. Davies, Structure–function relationships in calpains, Biochem. J. 447 (3) (Nov. 2012) 335–351, https://doi.org/10.1042/BJ20120921.
[8] H. Nian, B. Ma, Calpain–calpastatin system and cancer progression, Biol. Rev. 96 (3) (Jun. 2021) 961–975, https://doi.org/10.1111/brv.12686.
[9] H. Sorimachi, H. Mamitsuka, Y. Ono, Understanding the substrate specificity of conventional calpains, Biol. Chem. 393 (9) (Sep. 2012) 853–871, https://doi.org/10.1515/hsz-2012-0143.
[10] V. Briz, M. Baudry, Calpains: master regulators of synaptic plasticity, Neuroscientist 23 (3) (Jun. 2017) 221–231, https://doi.org/10.1177/1073858416649178.
[11] T. Miyazaki, R. Akasu, A. Miyazaki, Calpain-associated proteolytic regulation of the stromal microenvironment in cancer, CPD 27 (28) (Sep. 2021) 3128–3138, https://doi.org/10.2174/1381612827666210311143053.

[12] E.R. García-Trevijano, E. Ortiz-Zapater, A. Gimeno, J.R. Viña, R. Zaragozá, Calpains, the proteases of two faces controlling the epithelial homeostasis in mammary gland, Front. Cell Dev. Biol. 11 (Sep. 2023) 1249317, https://doi.org/10.3389/fcell.2023.1249317.
[13] Y.M. Patel, M.D. Lane, Role of calpain in adipocyte differentiation, Proc. Natl. Acad. Sci. USA. 96 (4) (Feb. 1999) 1279–1284, https://doi.org/10.1073/pnas.96.4.1279.
[14] Y.M. Patel, M.D. Lane, Mitotic clonal expansion during preadipocyte differentiation: calpain-mediated turnover of p27, J. Biol. Chem. 275 (23) (Jun. 2000) 17653–17660, https://doi.org/10.1074/jbc.M910445199.
[15] L. Muniappan, et al., Calpain inhibition attenuates adipose tissue inflammation and fibrosis in diet-induced Obese mice, Sci. Rep. 7 (1) (2017) 14398, https://doi.org/10.1038/s41598-017-14719-9. Oct.
[16] Y. Yajima, M. Sato, H. Sorimachi, M. Inomata, M. Maki, S. Kawashima, Calpain system regulates the differentiation of adult primitive mesenchymal ST-13 adipocytes, Endocrinology 147 (10) (Oct. 2006) 4811–4819, https://doi.org/10.1210/en.2005-1647.
[17] Q.-Q. Tang, T.C. Otto, M.D. Lane, Mitotic clonal expansion: a synchronous process required for adipogenesis, Proc. Natl. Acad. Sci. USA. 100 (1) (Jan. 2003) 44–49, https://doi.org/10.1073/pnas.0137044100.
[18] Z. Qiu, Y. Wei, N. Chen, M. Jiang, J. Wu, K. Liao, DNA synthesis and mitotic clonal expansion is not a required step for 3T3-L1 preadipocyte differentiation into adipocytes, J. Biol. Chem. 276 (15) (Apr. 2001) 11988–11995, https://doi.org/10.1074/jbc.M011729200.
[19] K. Zebisch, V. Voigt, M. Wabitsch, M. Brandsch, Protocol for effective differentiation of 3T3-L1 cells to adipocytes, Anal. Biochem. 425 (1) (Jun. 2012) 88–90, https://doi.org/10.1016/j.ab.2012.03.005.
[20] W. Guo, et al., Adipogenesis licensing and execution are disparately linked to cell proliferation, Cell Res. 19 (2) (Feb. 2009) 216–223, https://doi.org/10.1038/cr.2008.319.
[21] X. Zhao, et al., A comparison of methods for effective differentiation of the frozen-thawed 3T3-L1 cells, Anal. Biochem. 568 (Mar. 2019) 57–64, https://doi.org/10.1016/j.ab.2018.12.020.
[22] D.L. Brasaemle, T. Barber, N.E. Wolins, G. Serrero, E.J. Blanchette-Mackie, C. Londos, Adipose differentiation-related protein is an ubiquitously expressed lipid storage droplet-associated protein, J. Lipid Res. 38 (11) (Nov. 1997) 2249–2263.
[23] U.-J.P. Zimmerman, W.W. Schlaepfer, Two-stage autolysis of the catalytic subunit initiates activation of calpain I, Biochim. Biophys. Acta Protein Struct. Mol. Enzymol. 1078 (2) (Jun. 1991) 192–198, https://doi.org/10.1016/0167-4838(91)99009-H.
[24] J.S. Chou, F. Impens, K. Gevaert, P.L. Davies, m-Calpain activation in vitro does not require autolysis or subunit dissociation, Biochim. Biophys. Acta, Proteins Proteomics 1814 (7) (Jul. 2011) 864–872, https://doi.org/10.1016/j.bbapap.2011.04.007.
[25] R.A. Hanna, R.L. Campbell, P.L. Davies, Calcium-bound structure of calpain and its mechanism of inhibition by calpastatin, Nature 456 (7220) (Nov. 2008) 409–412, https://doi.org/10.1038/nature07451.
[26] T. Arnandis, et al., Calpains mediate epithelial-cell death during mammary gland involution: Mitochondria and lysosomal destabilization, Cell Death Differ. 19 (9) (Sep. 2012) 1536–1548, https://doi.org/10.1038/cdd.2012.46.
[27] T. Arnandis, et al., Differential functions of calpain 1 during epithelial cell death and adipocyte differentiation in mammary gland involution, Biochem. J. 459 (2) (Apr. 2014) 355–368, https://doi.org/10.1042/BJ20130847.
[28] Q.-Q. Tang, M.D. Lane, Activation and centromeric localization of CCAAT/enhancer-binding proteins during the mitotic clonal expansion of adipocyte differentiation, Genes Dev. 13 (17) (Sep. 1999) 2231–2241, https://doi.org/10.1101/gad.13.17.2231.
[29] Q.Q. Tang, M.D. Lane, Adipogenesis: from stem cell to adipocyte, Annu. Rev. Biochem. 81 (1) (Jul. 2012) 715–736, https://doi.org/10.1146/annurev-biochem-052110-115718.
[30] Y.K. Lee, Y.S. Chung, J.H. Lee, J.M. Chun, J.H. Park, The intricate role of p53 in adipocyte differentiation and function, Cells 9 (12) (Dec. 2020) 2621, https://doi.org/10.3390/cells9122621.
[31] X. Li, et al., An intronic enhancer of *Cebpa* regulates adipocyte differentiation and adipose tissue development via long-range loop formation, Cell Prolif. 57 (3) (Mar. 2024) e13552, https://doi.org/10.1111/cpr.13552.
[32] M. Baer, S.C. Williams, A. Dillner, R.C. Schwartz, P.F. Johnson, Autocrine signals control CCAAT/enhancer binding protein beta expression, localization, and activity in macrophages, Blood 92 (11) (Dec. 1998) 4353–4365.
[33] M. Dhaenens, P. Glibert, P. Meert, L. Vossaert, D. Deforce, Histone proteolysis: a proposal for categorization into “clipping” and “degradation”, Bioessays 37 (1) (Jan. 2015) 70–79, https://doi.org/10.1002/bies.201400118.
[34] M.D. Lane, Q.-Q. Tang, M.-S. Jiang, Role of the CCAAT enhancer binding proteins (C/EBPs) in adipocyte differentiation, Biochem. Biophys. Res. Commun. 266 (3) (Dec. 1999) 677–683, https://doi.org/10.1006/bbrc.1999.1885.
[35] M.H.G. Kubbutat, K.H. Vousden, Proteolytic cleavage of human p53 by calpain: a potential regulator of protein stability, Mol. Cell Biol. 17 (1) (Jan. 1997) 460–468, https://doi.org/10.1128/MCB.17.1.460.
[36] Y. Zhang, et al., Phosphorylation prevents C/EBPβ from the calpain-dependent degradation, Biochem. Biophys. Res. Commun. 419 (3) (Mar. 2012) 550–555, https://doi.org/10.1016/j.bbrc.2012.02.058.
[37] H. Zheng, W. Xie, The role of 3D genome organization in development and cell differentiation, Nat. Rev. Mol. Cell Biol. 20 (9) (Sep. 2019) 535–550, https://doi.org/10.1038/s41580-019-0132-4.
[38] G.K. Azad, S. Swagatika, M. Kumawat, R. Kumawat, R.S. Tomar, Modifying chromatin by histone tail clipping, J. Mol. Biol. 430 (18) (Sep. 2018) 3051–3067, https://doi.org/10.1016/j.jmb.2018.07.013.
[39] F. Shinkai-Ouchi, M. Shindo, N. Doi, S. Hata, Y. Ono, Calpain-2 participates in the process of calpain-1 inactivation, Biosci. Rep. 40 (11) (Nov. 2020), https://doi.org/10.1042/BSR20200552. BSR20200552.
[40] K. Ojima, S. Hata, F. Shinkai-Ouchi, Y. Ono, S. Muroya, Calpain-3 not only proteolyzes calpain-1 and -2 but also is a substrate for calpain-1 and -2, J. Biochem. 174 (5) (Oct. 2023) 421–431, https://doi.org/10.1093/jb/mvad057.